Energy barriers, structure, and two-stage melting of microclusters of vortices

Yu. E. Lozovik* and E. A. Rakoch
Institute of Spectroscopy, Russian Academy of Sciences, Troitsk, Moscow region, 142092 Russia
(Received 7 August 1997)

The melting of two-dimensional microclusters of ''particles'' with logarithmic repulsive interaction and confined by an external parabolic potential is considered. The model describes the behavior of vortices in a small island or grain of a type-II superconductor with a thickness smaller than the coherent length, vortices in a rotating vessel with superfluid, or electrons in a semiconductor nanostructure, surrounded by a media with a dielectric constant essentially smaller than that for the nanostructure. Shell configurations corresponding to the local and global minima of the potential energy for microclusters (''Periodic Table'' for a two-dimensional Thomson atom) are calculated, image potentials being taken into account. Due to image forces, configurations with larger numbers of vortices in internal shells become more stable. Rearrangements of the structure due to the anisotropy of confinement are studied. By the analysis of the temperature dependence of structure, radial, and angular rms displacements, the melting of clusters is analyzed. Two-stage melting of microclusters of vortices takes place: at lower temperature *rotatory reorientation of neighboring ''crystalline'' shells (''orientational melting'') arises;* at much greater temperatures the radial shell order disappears. Two-stage melting is connected with the fact that barrier of shell rotation U_2 is less than the barrier of intershell particle jump U_1, the ratio U_2/U_1 drops essentially for small microclusters. For clusters with a larger number of particles, orientational melting takes place only for external pairs of shells. This last fact is connected with approximate equality of barriers $U_1 \approx U_2$ for inner shells. [S0163-1829(98)00101-5]

I. INTRODUCTION.

The magnetic field H at $H_{c_2} > H > H_{c_1}$ penetrates into the type-II superconductors as Abrikosov vortices, which must form in a low-temperature region (in the absence of centers of pinning) an ideal triangular lattice.[1] The melting of the vortex lattice and formation of a liquid vortex phase with the increase of temperature may take place. This effect was observed for high-T_c superconductors (see review, Ref. 2, and references therein).

A very interesting problem arises concerning the structure of the mesoscopic system with a *small* number of vortices in a superconducting island or grain. Such a system may be considered as a two-dimensional analog (compare with Ref. 3) of a classical Thomson atom.[4] The latter system obeys laws of two-dimensional (2D) electrostatics. This model can describe also vortices in a rotating vessel with superfluid, or electrons in a semiconductor dot surrounded by a substance with an essentially smaller dielectric constant than that in the dot. A small system of vortices must behave as a *microcluster*. It means that a shell structure of the microcluster of vortices may abruptly change when we add only one vortex (one ''particle'') to the system. This structural sensitivity to the number N of particles takes place until N achieves some value $N_{\rm cr}$, when inside the cluster appears a region with a structure similar to that of the infinite phase (i.e., triangular lattice for 2D system). In other words at $N > N_{\rm cr}$ the transition from microcluster to a *macrocluster* of vortices must take place (at much greater number N, for ''*microparticles*,'' the number of vortices in the ''volume'' phase becomes greater than the number of ''surface'' vortices). The most interesting fact is that the melting of the microcluster may have interesting specific features in comparison with the melting of the macroscopic phase.[3,5–7]

In the present paper we study changes of the structure with temperature and the melting of microclusters of vortices in axial-symmetric systems. Microclusters of vortices have a shell structure. The analog of the Periodic Table for a two-dimensional Thomson atom is found. It is shown that *the melting of a 2D microcluster of vortices takes place in two stages* for small N, in the first stage intershell (''orientational'') melting takes place, and at an essentially higher temperature the shell structure disappears. It occurs that two-stage melting for small microclusters is connected with the fact that barriers of intershell rotation are smaller than barriers of jumps of particles between shells. We found that for microclusters consisting of two shells the ratio of potential barriers corresponding to the relative rotation of shells and to jumps of particles is much smaller than this value for clusters with more than two shells. That is why the ratio of orientational and total melting temperatures is much smaller for microclusters than for studied macroclusters. For internal shells of macroclusters this ratio has the order of 1 and the orientational melting takes place only for external shells.

The paper is organized as follows. In Sec. II we describe physical realizations of logarithmic clusters. Section III is devoted to configurations of vortex clusters in global and local minima of the potential energy and to the study of competition between the shell structure and the triangular lattice when the number of particles is growing. In Sec. IV results of the calculation of the intershell and the total melting of the vortex clusters are presented. In Sec. V the potential barriers of the relative rotation of shells and barriers for jumps of particles from one shell to another are analyzed. We take into account image potentials in Sec. VI. Section VII is devoted to the confinement anisotropy effects. Conclusions are presented in Sec. VIII.

II. PHYSICAL MODEL

Let us consider an island of the type-II superconductor in a normal magnetic field. If the thickness of the island d is smaller than the length of coherence $\xi(T)$ of the superconductor, then from the point of view of the superconductive properties the island at temperature T may be considered as the *two-dimensional* one. The magnetic field penetrates into the system as two-dimensional (2D) vortices. The potential of the interaction between two 2D vortices has the form (see Ref. 8)

$$U(r) = -q^2 \ln\frac{r}{a}, \quad a \ll r \ll \lambda_\perp ,$$

$$U(r) = -q^2 \frac{\lambda_\perp}{r} + \text{const}, \quad r \gg \lambda_\perp , \tag{1}$$

where q is the vortex ''charge,'' which is proportional to the superfluid density; r is a distance between the vortices; a is a radius of the core of a vortex, $a \sim \xi(T)$; $\lambda_\perp = \lambda^2/d$ is the penetration depth of the normal magnetic field in a 2D superconductor, λ is the London penetration depth of the magnetic field into a three-dimensional superconductor. For example, one has $\lambda_\perp \simeq 4$ μm for islands with the thickness $d \simeq 100$ Å and for $\lambda \simeq 2000$ Å.

Suppose that the radius of the superconductive island obeys the inequality $\xi \ll R \ll \lambda_\perp$. In this case one can consider the vortices as point particles which repulse under the logarithmic law. Stabilization of the concentration of vortices in superconductors in external magnetic field is taken into account in this model by the effective external confining potential $U_{\text{ext}}(r) = \alpha r_i^2$ or equivalently by homogeneous compensating incompressible background charge $\rho(r) = -2\alpha = -\rho_{\text{vortex}}$. It occurs that image forces for vortices (see below) as a rule do not change *qualitatively* the basic properties of the system.

So in the first approximation we have a model of the two-dimensional (2D) cluster of N classical particles repelling from each other due to the logarithmic law $U(r_{ij}) = -q^2 \ln(r_{ij}/a)$ (i.e., obeyed to 2D electrostatics law) and confined by the external potential $U_{\text{ext}}(r_i) = \alpha r_i^2$.

After the scaling transformations $r \to \alpha^{1/2} qr$; $T \to (k_B/q^2)T$; $U \to (1/q^2)U$ the potential energy of the system [measured from the $C_N^2 \ln(q/\alpha^{1/2}a)$] is:

$$U = -\sum_{i>j} \ln\frac{r_{ij}}{a} + \sum_i r_i^2 . \tag{2}$$

We show that properties of clusters change qualitatively only at sufficiently great anisotropy of $U_{\text{eff}}(r)$.

The system of classical particles with the potential (2) is a two-dimensional analog of the classical three-dimensional (3D) Thomson atom.[4,9] Such a model approximately describes not only vortices in a superconductive island, but also vortices in a *rotating vessel* with superfluid He (see Refs. 10–15). It also describes a cluster of electrons or holes in a semiconductor nanostructure (2D dot), surrounded by a media with a dielectric constant ϵ essentially smaller than that ($\epsilon_{q\text{dot}}$) of the 2D dot. Effective logarithmic interaction take place at interelectron distances r such that $D \ll r \ll D/k$; D is the thickness of nanostructure, $k = \epsilon/\epsilon_{q\text{dot}}$; in this case image charges originated from polarization of media near the interface by carriers in the dot form charged lines (with the same charge sign of carriers in dot) and this leads to the effective logarithmic interaction between carriers. Note that image forces in the last case amplify interelectron effective repulsion in comparison with bare Coulomb interaction and this effect is favored for electron crystallization.

III. GROUND-STATE CONFIGURATIONS

By analogy with *three-dimensional* Coulomb system *without* external confining potential, but with external abrupt boundaries, all particles with the logarithmic potential of repulsion in 2D system must locate on the external (one-dimensional) boundary of the system. However in both systems equilibrium of charges *inside* the system is possible if a compensating incompressible charged background (or equivalent confining potential), discussed above, is present.

To study ground-state configurations of particles we used two methods: an accidental search of the minimum of the potential energy of the system and also Langevin dynamics. Both methods give very close results. It is convenient to use polygons inscribed into circles as initial configurations, i.e., clusters consisting of shells close to circles (see below). We alternated accidental movement of shells as a *whole* (at each step one shell chosen accidentally moved accidentally) and accidental movement of particles (at each step one particle chosen accidentally moved accidentally). A new configuration of particles was taken if after the next step the increase of the potential energy δU of the system was smaller then zero. The maximal value of the step was decreased from 5×10^{-3} to 1×10^{-6} in the dimensionless units. The step was decreased approximately 0.8–0.95 times every 10^3 steps.

We found local and global (deepest of local ones) minima of the potential. It occurs that small logarithmic clusters (analogously to Coulomb ones, see Refs. 3, 5–7) have shell structure at low temperatures. Shell structure of microclusters is connected with the axial (or almost axial) symmetry of confinement. As one knows, a 2D crystal has a triangular lattice. The region inside the cluster with triangular structure arises only for clusters with a large number of particles ($N \simeq 100$) as for Coulomb clusters[3,5,6]. Below we present the results of computer simulations of the structure of the logarithmic clusters.

Figure 1 reveals that the character of the dependence of the mean total, internal, and external potential energies per particle vs the number of particles is not far from linear one. Figure 1 shows smooth decreasing of mean total and internal potential energies vs number of particles N and the smooth increasing of external potential energy vs number of particles N. The total potential energy per particle E/N decreases vs N for $N \leqslant 50$.

In Table I the numbers of particles in shells and corresponding mean total potential energies [measured from the value $C_N^2 \ln(q/\alpha^{1/2}a)$, see above] are represented for the global minima. The subsequent filling of shells reminds one of the formation of the Periodic Table of elements (one can compare the filling of shells in the 2D classical system with 3D Coulomb interaction[3]). When $N \leqslant 5$ all particles locate in

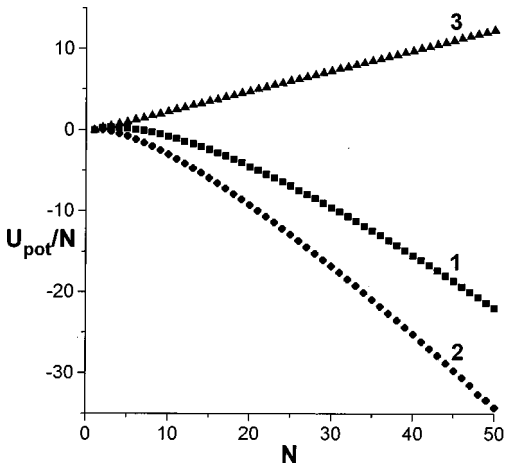

FIG. 1. Potential energy of two-dimensional vortex clusters per particle $\langle U_{\rm pot}\rangle/N$ as a function of number N of particles. (1) Indicates the total potential energy $\langle U_{\rm pot}\rangle/N$; (2) Indicates potential energy of all interactions between particles $\langle U_{\rm int}\rangle/N=(1/2N)\Sigma\langle U_{ij}\rangle$; (3) indicates the external potential energy $\langle U_{\rm ext}\rangle/N=1/N\,\alpha\Sigma r_i^2$.

one shell with the center at the center of the symmetry (at minimum of the confining potential) and the particles are in vertexes of a proper polygon. The number of particles on the different shells increases until the filling of each of them reaches some maximal value. For $N<50$, the central shell does not exceed five particles, the second shell does not exceed 11 particles [in the case of an ideal two-dimensional crystal the distribution of particles on coordinate circles corresponds to (1,6,12, . . .)]. When all the shells are filled up to their allowed maximal numbers of particles, a new shell appears: first only one new particle appears in the center of the system, then if one more particle is added two particles make the central shell, etc. One particle in the center appears only when we add one particle to the system which has the configuration (5, . . .), two particles appear near the center for the initial configuration (1,7, . . .) or (1,8, . . .), three particles—for the initial configuration (2,8, . . .), four particles—for (3,9, . . .), five particles—for (4,11, . . .). Analogous effects take place for Coulomb clusters.[3,6,7]

From the previous discussion one can see that we used the term ''shell'' not only in the case when it has a form of an equilateral polygon. In work Ref. 12, which is devoted to 2D clusters of vortices in a rotating vessel with superfluid helium, numbers of particles in the shells were determined with the help of the following criterion: two particles belong to the same shell if distances from them to the center of the system differed not more than 2% for $N<50$ and 5% for $N>50$. But this determination seems to be rather not convenient, because there is no universality for any number of particles. We use another definition of a shell. Let us deter-

TABLE I. Shell structure and potential energy of clusters of vortices.

Number of particles	Shell fillings	Potential energy	Number of particles	Shell fillings	Potential energy
1	1	0.000000×10^{0}	26	3,9,14	-1.940569×10^{2}
2	2	5.000000×10^{-1}	27	3,9,15	-2.156137×10^{2}
3	3	8.918023×10^{-1}	28	4,9,15	-2.384294×10^{2}
4	4	1.090457×10^{0}	29	4,10,15	-2.625912×10^{2}
5	5	9.764052×10^{-1}	30	4,10,16	-2.881028×10^{2}
6	1,5	4.354169×10^{-1}	31	4,10,17	-3.149268×10^{2}
7	1,6	-7.512442×10^{-1}	32	4,11,17	-3.431329×10^{2}
8	1,7	-2.514746×10^{0}	33	5,11,17	-3.727473×10^{2}
9	1,8	-4.914510×10^{0}	34	1,5,11,17	-4.037308×10^{2}
10	2,8	-8.100414×10^{0}	35	1,6,11,17	-4.361606×10^{2}
11	3,8	-1.209333×10^{1}	36	1,6,12,17	-4.700331×10^{2}
12	3,9	-1.697858×10^{1}	37	1,6,12,18	-5.053534×10^{2}
13	4,9	-2.271610×10^{1}	38	1,6,12,19	-5.420929×10^{2}
14	4,10	-2.942793×10^{1}	39	1,7,13,18	-5.803155×10^{2}
15	4,11	-3.706118×10^{1}	40	1,7,13,19	-6.200430×10^{2}
16	5,11	-4.573707×10^{1}	41	1,7,13,20	-6.612310×10^{2}
17	1,5,11	-5.541308×10^{1}	42	1,7,14,20	-7.039416×10^{2}
18	1,6,11	-6.620692×10^{1}	43	2,8,14,19	-7.481666×10^{2}
19	1,6,12	-7.811655×10^{1}	44	2,8,14,20	-7.939606×10^{2}
20	1,6,13	-9.110199×10^{1}	45	2,8,14,21	-8.412619×10^{2}
21	1,7,13	-1.052696×10^{2}	46	3,9,14,20	-8.901514×10^{2}
22	1,7,14	-1.205683×10^{2}	47	3,9,15,20	-9.406122×10^{2}
23	1,8,14	-1.370647×10^{2}	48	3,9,15,21	-9.926554×10^{2}
24	2,8,14	-1.548203×10^{2}	49	3,9,15,22	-1.046250×10^{3}
25	3,8,14	-1.737968×10^{2}	50	4,10,15,21	-1.101460×10^{3}
107	3,9,15,21,27,32	-7.155730×10^{3}			
108	3,9,15,21,27,33	-7.316694×10^{3}	192	3,9,15,21,27,33,39,45	-2.834568×10^{4}

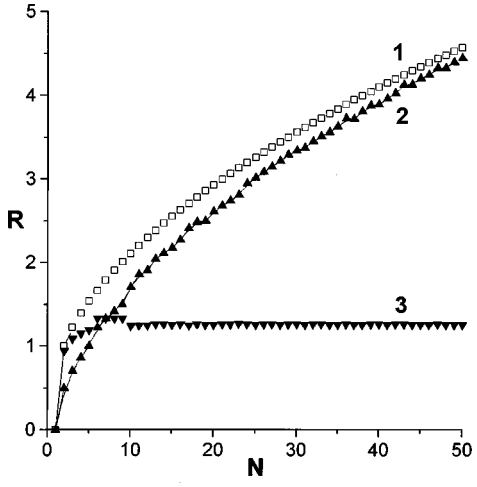

FIG. 2. The average distance between the particles r and the radius of the system R as a function of N particles. (1) The average distance between the particles; (2) The radius of the system; (3) the lattice period a.

mine a shell as a convex polygon with a maximal number of particles (inside of which the previous shell locates) which satisfies the following rule: the maximal distance from a particle of this shell to the center of the system has to be less than the minimal distance from a particle of a neighboring external shell to the center of the system (this rule changes in the case of anisotropical external potential—see Sec. VII). As a result, the filling of shells in clusters, which we obtain from our calculations, resembles the rules of filling of shells in Thomson atom[3,6,7]. In particular on increasing the number of particles, the number of shells cannot decrease, contrary to Ref. 12.

As the confining potential is central symmetric, one can expect for shells to be proper polygons which are inscribed into circles. But in some cases in microclusters with $N<50$ the spontaneous breaking of the axial symmetry takes place. It is most strongly revealed in clusters with two particles in the central shell [in 2D clusters with $N=10$ for the configuration (2,8) and with $N=24$ for the configuration (2,8,14)]. In last cases the central shell induces the form of an ellipse for the second shell.

An analytical calculation of radius and potential energy of the clusters consisting of one shell, or two shells with one particle in the center, confirms the accuracy ($\sim 10^{-9}$) of computer simulations.

Figure 2 shows that the average distance $\langle r \rangle$ between particles increases monotonously with an increase in the number of particles (derivative $d<r>/dN$ decreasing vs N). But the radius R of the system is not a monotonous function of N. If we compare Fig. 2 and Table I, we can see that the *radius of system the R increases sharply when a new shell appears* (when one added particle locates in the center), or when we add one particle to the central shell. If the cluster becomes more symmetric when we add only one particle then the radius of the system can *even decrease* a little, as we can see from Fig. 2. Not taking into account the mentioned fluctuations of the radius vs N, the size of the system increases approximately proportionally to $\sqrt{N}$. Lattice period a (see Sec. VI) takes approximately the constant value for $N>9$ (see Fig. 2). The last two facts demonstrate the approximate

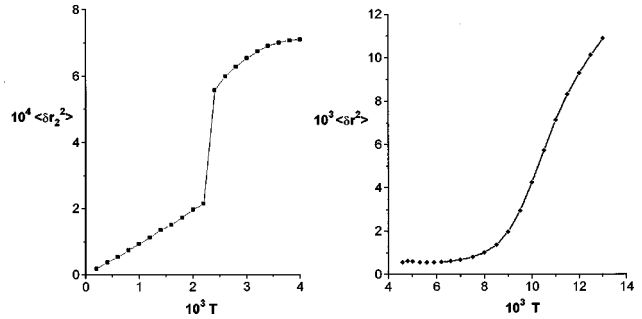

FIG. 3. The radial square deviation $\langle \delta r^2 \rangle$ as a function of temperature; $N=37$. (a) Low-temperature region. Radial square deviation of the middle shell. (b) High-temperature region. Total radial square deviation.

constancy of the density of particles.

It should be noted that the search of the global minimum configurations requires great large accuracy for large N (not less than 10^{-7} at $N\sim 50$ and not less than 10^{-8} at $N\sim 100$), because of the existence of a large number of local minima with energies very close to that of the global minimum. For example, at $N=49$ the difference in energy between the global minimum (3,9,15,22) and the local minimum (3,9,16,21) is only 4×10^{-4}% and at $N=107$ the difference between the global (3,9,15,21,27,32) and the local minimum (3,9,15,22,27,31) is only 5×10^{-5}%.

IV. MELTING AND PHASE TRANSITIONS

We used the Monte Carlo method with an accidental movement of shells as a whole and accidental movement of particles for studying different physical quantities as functions of temperature.

After ground-state configuration was achieved, the system was heated up to the temperature ΔT, which was typically from 1×10^{-7} to 5×10^{-3}, and equilibrated at this temperature during 4×10^4 Monte Carlo steps. Then physical quantities of the system were calculated by averaging over different (about $1\times 10^6 - 1\times 10^7$) Monte Carlo configurations. After this the system was heated up again to the new temperature ($\sim 2\Delta T$) using the described procedure, etc. We calculated the following quantities:

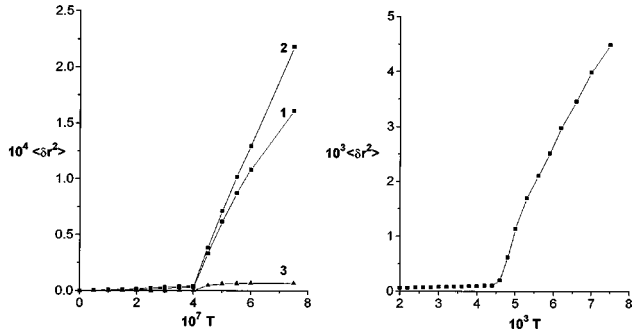

FIG. 4. The radial square deviation $\langle \delta r^2 \rangle$ as a function of temperature; $N=11$. (a) Low-temperature region. (1) Total radial square deviation; (2) Radial square deviation of the external shell; (3) radial square deviation of the internal shell. (b) High-temperature region.

TABLE II. Melting temperatures and potential barriers.

	T_c	Λ	$U_{1,2}$
$N=11$. Orientational melting of the external shell relative to the internal one.	4.0×10^{-7}	25×10^{5}	2.32×10^{-6}
$N=11$. Total melting.	4.5×10^{-3}	222	3.71×10^{-2}
$N=37$. Orientational melting of the external shell relative to the middle one.	8.0×10^{-4}	1250	2.30×10^{-3}
$N=37$. Orientational melting of the middle shell relative to the internal one.	2.4×10^{-3}	417	1.61×10^{-2}
$N=37$. Total melting.	8.0×10^{-3}	125	6.61×10^{-2}
$N=107$. Orientational melting of the external shell relative to the neighbor one.	7.5×10^{-3}	133	3.0×10^{-2}
$N=107$. Total melting.	8.5×10^{-3}	118	5.8×10^{-2}

(1) The total potential energy $U_{\rm pot}$.

(2) The total radial square deviation:

$$\langle \delta R^2\rangle = \frac{1}{N}\sum_{i=1}^{N}\frac{\langle r_i^2\rangle-\langle r_i\rangle^2}{a^2} \tag{3}$$

and radial square deviations for each shell:

$$\langle \delta r^2\rangle = \frac{1}{N_R}\sum_{i=1}^{N_R}\frac{\langle r_i^2\rangle-\langle r_i\rangle^2}{a^2}, \tag{4}$$

where N_R is a number of particles in the shell, a is the average distance between the particles, and $\langle\ \rangle$ denotes an average over Monte Carlo configurations.

(3) The relative angular intrashell square deviations

$$\langle \delta\phi_{\rm int}^2\rangle = \frac{1}{N_R}\sum_{i=1}^{N_R}\frac{\langle(\phi_i-\phi_{i_1})^2\rangle-\langle(\phi_i-\phi_{i_1})\rangle^2}{\phi_0^2} \tag{5}$$

and the relative angular intershell square deviations

$$\langle \delta\phi_{\rm ext}^2\rangle = \frac{1}{N_R}\sum_{i=1}^{N_R}\frac{\langle(\phi_i-\phi_{i_2})^2\rangle-\langle(\phi_i-\phi_{i_2})\rangle^2}{\phi_0^2}, \tag{6}$$

where i_1 and i_2 indicate the nearest particle from the same shell and from the nearest-neighbor shell, respectively, $2\phi_0=2\pi/N_R$ is the angular interelectron distance for the shell consisting of N_R particles. Only relative angular deviations are considered to exclude a rotation of the system as a whole.

The temperature dependence of the total radial square deviation is shown in Fig. 3(b) for $N=37$ and in Fig. 4(b) for $N=11$. The dependences of radial deviations on the temperature for all shells jump approximately at the same temperature $T=T_{c_1}$ (see Table II).

One can see from Figs. 5 and 6(b), that at the same temperature the relative angular intrashell square deviations for all shells also grow abruptly. It means, that at $T=T_{c_1}$ the cluster looses its ordered structure. At $T>T_{c_1}$ the number of particles in shells begin to change, shells begin to interchange by particles, and shell structure blurs out. At $T\gg T_{c_1}$

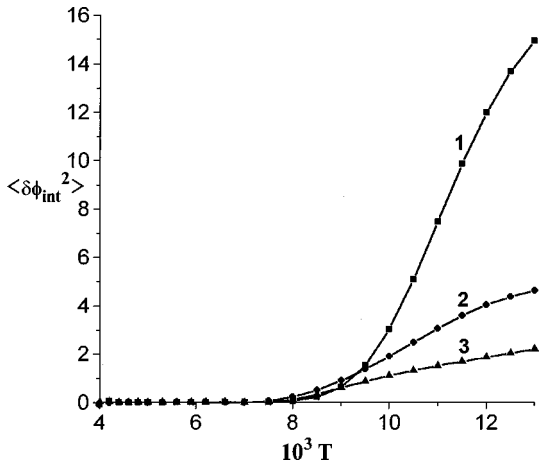

FIG. 5. The relative angular intrashell square deviation $\langle\delta\phi_1^2\rangle$ as a function of temperature; $N=37$. (1) Relative angular intrashell square deviation of the external shell. (2) Relative angular intrashell square deviation of the middle shell. (3) Relative angular intrashell square deviation of the internal shell.

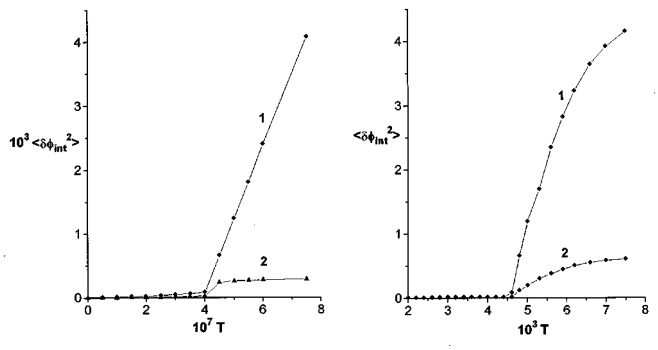

FIG. 6. The relative angular intrashell square deviation $\langle\delta\phi_1^2\rangle$ as a function of temperature; $N=11$. (a) Low-temperature region. (b) High-temperature region. (1) Relative angular intrashell square deviation of the external shell. (2) Relative angular intrashell square deviation of the internal shell.

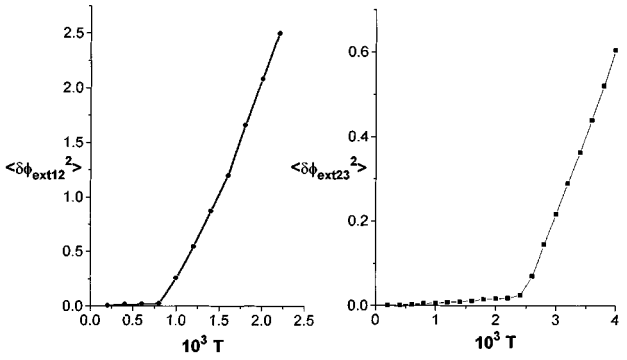

FIG. 7. The relative angular intershell square deviation $\langle \delta\phi_2^2 \rangle$ as a function of temperature; $N=37$. (a) Angular intershell square deviation of the middle shell relative to the external shell. (b) Angular intershell square deviation of the internal shell relative to the middle shell.

we cannot find any shell structure and the particles move chaotically. So we interpret T_{c_1} as the melting temperature of the cluster.

We found the values of the dimensionless parameter $\Lambda=\Lambda_{c_1}=q^2/k_B T_{c_1}$ (see Table II), corresponding to the melting of the system ($\Lambda=1/T$ for $q=k_B=1$). For $N=37$ the value of Λ_{c_1} does not differ significantly from the value Λ_c, when the melting of the system with a large number of vortices takes place ($\Lambda=\Lambda_c\simeq 130$). But, e.g., for $N=11$ the value of $\Lambda_{c_1}=220>\Lambda_c$, which is connected with a greater role of the parabolic confinement for small N, the circular-like structure wins in the competition with 2D triangle lattice.

One can see that the relative angular *intershell* square deviations as functions of temperature *jump at much lower temperature.* The dependences of the relative angular intershell square deviation from temperature for different pairs of shells break at different temperatures T_{c_2} (see Figs. 7, 8, and Table II). Thus at $T=T_{c_2}$ neighboring shells *being ''crystalline'' inside* and almost keeping their shape *rotated relatively with each other*. Intershell accidental rotation (reorientation) gives rise to the radial and intrashell angular displacements. The last fact is more noticeable for small

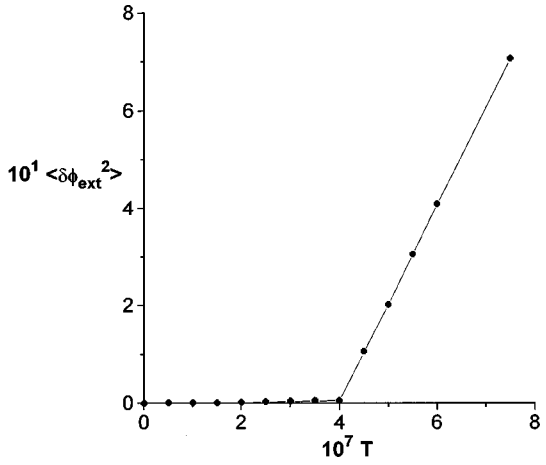

FIG. 8. The relative angular intershell square deviation $\langle \delta\phi_2^2 \rangle$ as a function of temperature; $N=11$.

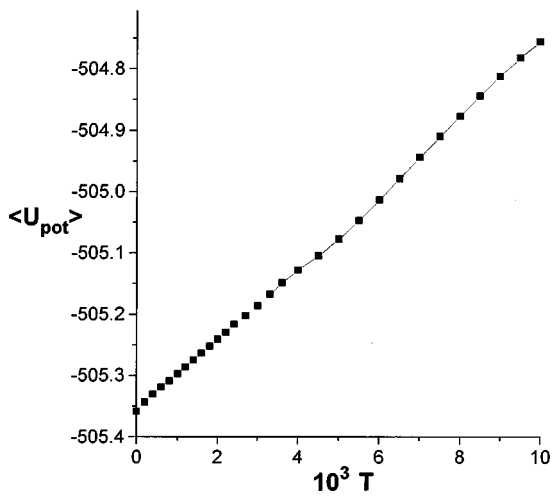

FIG. 9. Total potential energy $\langle U_{\rm pot} \rangle$ of a two-dimensional vortex cluster as a function of temperature; $N=37$.

clusters and for internal shells of large clusters with high symmetry. For example, from Figs. 4(a) and 6(a) one can see that radial deviations and relative angular intrashell deviations grow abruptly for all shells of cluster with $N=11$ at the temperature T_{c_2}, and from Fig. 3(a) one can see that radial deviation for the second shell in a cluster with $N=37$ slightly jumps at the temperature $T=T_{c_2}$. So *orientational melting* at the $T=T_{c_2}$ for corresponding pairs of shells takes place (this phenomena seems to be typical for microclusters with a shell structure and for small number of particles).

We also studied temperature dependences of radial and relative angular intrashell and intershell deviations for $N=107$ and found that they jump approximately simultaneously at $T_{c_1}=8.5\times 10^{-3}$. Only the dependence of relative angular intershell deviation of the external shell relative to the previous one jumps at lower temperature $T_{c_2}=7.5\times 10^{-3}$. So orientational melting for $N=107$ takes place only for the external pair of shells which are connected with the triangular structure of the internal region of macroclusters.

The typical values of the parameter Λ, relating to the orientational melting for different pairs of shells are much greater than that for the total melting for microclusters and have the same order for macroclusters (see Table II).

One can see from Fig. 9 that the dependence of the potential energy vs temperature increases almost linearly and smoothly (e.g., for cluster $N=37$). That is why we cannot use this dependence for the search of the melting temperature.

V. POTENTIAL BARRIERS FOR INTERSHELL ROTATION AND FOR JUMP OF A PARTICLE FROM ONE SHELL TO ANOTHER

The rotation of shells is the lowest excitation in the case of small clusters. The simplest estimation for the barrier for intershell rotation may be obtained (taking into account the essential ''relaxation'' of particles due to the rotation of shells) using the following procedure. Let us initially fix all particles of the cluster except particles in one shell and rotate

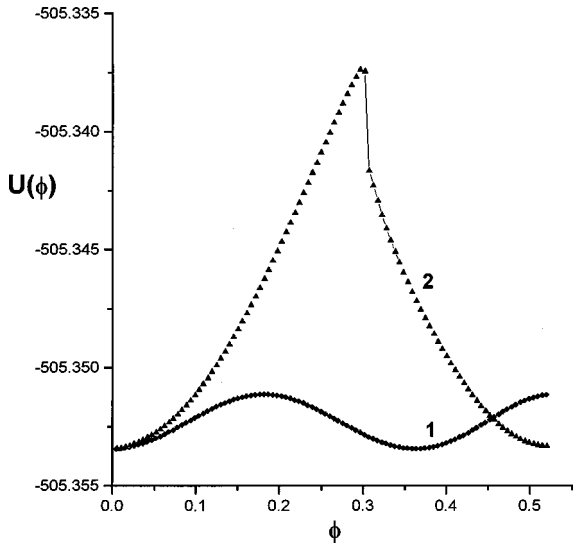

FIG. 10. Total potential energy U_{pot} of a two-dimensional vortex cluster as a function of the angle of shells rotation; $N=37$. (1) The external shell rotates relative to the middle one; (2) The middle shell rotates relatively to the internal one.

the last shell relative to other shells on the angle $\delta\phi$. Then let us fix only the angle ϕ_1 of one particle from a rotating shell and the angle ϕ_2 of one particle from the neighboring ''resting'' shell. After that we find the minimum of the potential energy for other $(2N-2)$ variables [N variable radii r and $(N-2)$ variable angles ϕ] by the accidental search method or by Langevin dynamics. Both methods give very close results. Let us remember the minimal potential energy of the system at fixed ϕ_1 and ϕ_2. Then we shall repeat this procedure, changing $\phi=\phi_1-\phi_2$ until one shell will rotate relative to another at the angle 2π. So we calculate the total potential energy U as a function of a rotating angle ϕ of one shell and the potential barrier of rotation.

The calculated dependence of the potential energy U on the angle of relative revolution of shells for clusters consisting of two shells ϕ may be approximated by the simple expression

$$U=\frac{U'}{2}\left[1-\cos\left(\frac{2\pi\phi}{\phi'}\right)\right], \tag{7}$$

where U' and ϕ' are the barrier height and the period, respectively. But for larger N this dependence is more complicated (see Fig. 10).

For comparison one can find also the potential barrier for a jump of a particle from one shell to another which is connected with the radial (total) melting of shells. Let us use the following procedure for its calculation. Let us initially fix all particles of the cluster except one particle (M) at the configuration which corresponds to the global minimum of the potential energy and let us move this particle M in the direction of its position at the local minimum of the potential energy at a radial step δr. Then we fix a final distance r from this particle to the center of the system and find the minimum of the total potential energy of the system as a function of $(2N-1)$ variables [$(N-1)$ variables r and N variables ϕ] by the accidental search method or by Langevin dynamics. Let us remember the minimal potential energy of this system

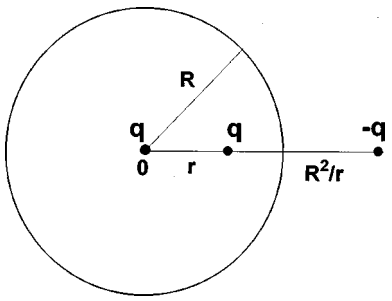

FIG. 11. Image charges.

at fixed r. Then we shall repeat this procedure until the system will have the configuration of the local minimum of the potential energy. So one can find the dependence of potential energy from coordinate r of the particle (which changes its own shell to another one) and so we find the potential barrier of the jump of the particle.[16]

We found the potential barriers for rotation U_2 and for a jump of a particle from one shell to another U_1 by the methods described above for the cluster $N=11$ [in the global minimum the cluster has the configuration (3,8), and in the local minimum—the configuration (2,9)] and for the cluster $N=37$ [in the global minimum the cluster has the configuration (1,6,12,18), in the local minimum—the configuration (1,7,12,17)] and for the cluster $N=107$ [in the global minimum the cluster has the configuration (3,9,15,21,27,32), and in the local minimum—the configuration (3,9,15,22,27,31)]. It is shown that orientational barriers are essentially less than the radial ones (see Table II) for $N=11,37$ and are slightly less for $N=107$. This fact along with the jump of the relative angular intershell deviation is the argument for the possibility of orientational melting in 2D microclusters of vortices.

The ratios of potential barriers of rotation and jump are equal in order of value to the ratios of temperatures of orientational and total melting for the same number of particles $(U_2/U_1\sim T_{c_2}/T_{c_1})$. Besides, the ratio of potential barriers of rotation for different pairs of shells is proportional to the ratio of temperatures of orientational melting for these pairs of shells (see Table II). These facts lead to the conclusion that two-stage melting in shell microclusters has the origin in the great difference between barriers of shell reorientation and intershell one-particle exchange (analogous situation takes place for Coulomb microclusters where orientational melting occurs, see Ref. 6). This gives one the possibility of predicting the existence of two-stage melting in shell clusters.

VI. IMAGE POTENTIAL EFFECTS

Now we shall investigate the influence of image potentials on the structure and on the melting of vortex clusters. Potential energies of the vortex system in a vessel with neutral superfluid or in superconductor island with small radius R ($\xi<R<\lambda_\perp$, see Sec. II) may be found from the solution of a two-dimensional Laplace equation with zero boundary conditions. So the interaction of vortices with the border reduces to the interaction of vortices with their own images and with images of other vortices.

It is easy to show that if a vortex with charge q is located at the point (r,α), then its image charge $-q$ is located at the

point $(R^2/r,\alpha)$ and in the center of a circular system (see Fig. 11). In this case the resulting potential obeyed the Laplace equation and the boundary conditions.

The potential energy of the vortex cluster taking into account all interactions including interactions of vortices with ''own'' and ''neighboring'' images has the form

$$U=\frac{q^2}{2}\left[\sum_i \sum_{j<i} \ln\frac{u_i^2u_j^2+1-2u_iu_j\cos(\phi_i-\phi_j)}{u_i^2+u_j^2-2u_iu_j\cos(\phi_i-\phi_j)} + \sum_i \ln(1-u_i^2)+n\ln\frac{R}{a}\right]+\alpha R^2\sum_i u_i^2, \tag{8}$$

where $u_i=r_i/R$.

After scaling transformations and omitting the term, which does not depend on r_i, one has the following expression for the potential energy:

$$U=\frac{1}{2}\sum_i \sum_{j<i} \ln\frac{u_i^2u_j^2+1-2u_iu_j\cos(\phi_i-\phi_j)}{u_i^2+u_j^2-2u_iu_j\cos(\phi_i-\phi_j)} + \frac{1}{2}\sum_i \ln(1-u_i^2)+R^2\sum_i u_i^2+\frac{1}{2}n\ln R. \tag{9}$$

Neglecting the image charges yields the potential energy in the form (2).

We calculated equilibrium structure of vortex clusters by taking into account image forces for $N=1,\ldots,50$, and taking the parameter R according to the following rule.

We introduced the effective radius of cluster $R_0=R_{\rm ext}+(R_{\rm ext}-R_{\rm mid})/2$, where $R_{\rm ext}$ is an average radius of the external shell and $R_{\rm mid}$ is that of the neighboring shell (in a cluster consisting of one shell $R_{\rm mid}=0$). The procedure described above is fulfilled without taking into account image charges. Then we calculated the average distance between neighboring particles in the cluster, i.e., lattice period a:

$$a=\frac{1}{\sqrt{\rho}}=\frac{\sqrt{\pi}R_0}{\sqrt{N}}, \tag{10}$$

where ρ is the particle density in the cluster. The dependence $a(N)$ is presented in Fig. 2. After that for simplicity we choose the parameter R [a new size of the cluster which enters the expression for the potential energy (9)] to be equal to $R=R_0+a$.

In Table III we give radii of clusters, total potential energies, and also parts of potential energies, calculated according to Eq. (2) (i.e., without image potentials). The configurations in the global minima for R chosen as above are the same as without taking into account image charges. All configurations corresponding to the local and global minima of the potential energy for $N=1,\ldots,50$ are studied, and as a result we revealed the following effect of the image potentials. The configurations with a larger number of vortices in internal shells become more stable (i.e., corresponding minima become deeper). So, for example, in a cluster with 45 particles rearrangement of shell structure due to image potentials takes place: a local minimum with a larger numbers of vortices in the internal shell (3,8,14,20) becomes a global minimum instead of the (2,8,14.21) configuration. Such a rearrangement can take place for some N, when in the first approximation (with omitted image potentials) potential energies in the global and in the nearest local minimum begin to differ a little, the larger number of particles in the internal shells being in the local minimum rather than the global one (e.g., for $N=20$). However energies in different minima coincide very seldom. So almost all configurations in the global minima do not change at fixed N and varying R (see Table III).

Note, that the part of the potential energy corresponding to Eq. (2) increases when image potentials are taken into account. This is connected with an increase of the average distance between particles, which occurs due to the attraction of particles to the boundary of a cluster, i.e., to own image charges. The role of image potentials decreases for large values of R. Near the cluster boundary repulsion of vortices weakens due to the attraction of vortices to image charges of partners. Because of the attraction of vortices to the center of the cluster they tend to compress near the center.

We investigated the melting of clusters with 37 and 11 particles with the interaction modified by image forces. We found that the character of melting does not change. One can also observe two-stage melting connected with jumps of radial and angular deviations. But the temperatures of orientational and total melting change a little in comparison with unmodified interaction. Really, e.g., in the case of clusters, consisting of 37 particles, the temperatures of orientational and total melting become closer, but in the case of 11 particles they *move away* (see Table IV). The matter is that in a cluster with 37 particles the configuration of the system in the global minimum is (1,6,12,18), and that in the local one is (1,7,12,17), i.e., in the local minimum in comparison with the global one more particles locate in the internal shell. That is why the difference in energy between the local and the global minima decreases if image charges are taken into account. Consequently the radial barrier for a jump of particles between these minima decreases. Therefore the ratio between total and orientational melting temperatures decreases.

The opposite situation occurs in clusters with 11 particles. In this case in the global minimum (3,8) in comparison with the local one (2,9) more particles are in the internal shell. Consequently the difference between the potential energies in local and global minima increases due to image potentials, and the ratio of total and orientational melting temperatures increases.

We have also calculated potential barriers relative to a rotation of shells and to a jump of particles between shells for $N=37$ and 11 (see Table IV). We found that image potentials decrease the difference of potential barriers of rotation of shells and that of the jump of a particle between shells in the case of cluster with 37 particles. However, the corresponding value increases for the cluster with 11 particles in accordance with the results of the melting simulations (compare Tables II and IV).

VII. INFLUENCE OF CONFINEMENT ANISOTROPY

Above we considered the central-symmetrical confinement $U_{\rm ext}=\Sigma_i r_i^2$. In this section we shall consider the anisotropic confinement

TABLE III. Shell structure and potential energy of clusters of vortices with image potentials being taken into account.

Number of particles	Cluster radius	Shell fillings	Potential energy U_{pot}	U [Eq. (2)]
2	1.690	2	2.066243×10^{0}	5.002660×10^{-1}
3	2.147	3	5.474305×10^{0}	8.918136×10^{-1}
4	2.452	4	1.005901×10^{1}	1.090458×10^{0}
5	2.689	5	1.581382×10^{1}	9.764053×10^{-1}
6	3.166	1,5	2.463708×10^{1}	4.354170×10^{-1}
7	3.313	1,6	3.278862×10^{1}	-7.512442×10^{-1}
8	3.450	1,7	4.206671×10^{1}	-2.514746×10^{0}
9	3.579	1,8	5.246424×10^{1}	-4.914510×10^{0}
10	3.461	2,8	6.018420×10^{1}	-8.100226×10^{0}
11	3.586	3,8	7.219065×10^{1}	-1.209331×10^{1}
12	3.690	3,9	8.485980×10^{1}	-1.697854×10^{1}
13	3.820	4,9	9.924647×10^{1}	-2.271610×10^{1}
14	3.911	4,10	1.137701×10^{2}	-2.942793×10^{1}
15	3.998	4,11	1.292338×10^{2}	-3.706116×10^{1}
16	4.114	5,11	1.466207×10^{2}	-4.573707×10^{1}
17	4.141	1,5,11	1.619900×10^{2}	-5.541307×10^{1}
18	4.265	1,6,11	1.818184×10^{2}	-6.620691×10^{1}
19	4.341	1,6,12	2.008231×10^{2}	-7.811655×10^{1}
20	4.411	1,6,13	2.205592×10^{2}	-9.110199×10^{1}
21	4.521	1,7,13	2.432477×10^{2}	-1.052696×10^{2}
22	4.586	1,7,14	2.647526×10^{2}	-1.205683×10^{2}
23	4.691	1,8,14	2.895335×10^{2}	-1.370647×10^{2}
24	4.736	2,8,14	3.117367×10^{2}	-1.548200×10^{2}
25	4.788	3,8,14	3.351895×10^{2}	-1.737967×10^{2}
26	4.886	3,9,14	3.627600×10^{2}	-1.940568×10^{2}
27	4.944	3,9,15	3.884959×10^{2}	-2.156120×10^{2}
28	4.994	4,9,15	4.145146×10^{2}	-2.384292×10^{2}
29	5.088	4,10,15	4.451034×10^{2}	-2.625902×10^{2}
30	5.145	4,10,16	4.735792×10^{2}	-2.881023×10^{2}
31	5.199	4,10,17	5.028077×10^{2}	-3.149267×10^{2}
32	5.286	4,11,17	5.360194×10^{2}	-3.431325×10^{2}
33	5.335	5,11,17	5.665284×10^{2}	-3.727471×10^{2}
34	5.385	1,5,11,17	5.980214×10^{2}	-4.037297×10^{2}
35	5.434	1,6,11,17	6.302268×10^{2}	-4.361595×10^{2}
36	5.518	1,6,12,17	6.675049×10^{2}	-4.700330×10^{2}
37	5.567	1,6,12,18	7.015965×10^{2}	-5.053534×10^{2}
38	5.616	1,6,12,19	7.368547×10^{2}	-5.420927×10^{2}
39	5.696	1,7,13,18	7.767003×10^{2}	-5.083153×10^{2}
40	5.743	1,7,13,19	8.133019×10^{2}	-6.200425×10^{2}
41	5.788	1,7,13,20	8.505012×10^{2}	-6.612302×10^{2}
42	5.864	1,7,14,20	8.933134×10^{2}	-7.039416×10^{2}
43	5.913	2,8,14,19	9.330197×10^{2}	-7.486212×10^{2}
44	5.957	2,8,14,20	9.727602×10^{2}	-7.939598×10^{2}
45	6.003	3,8,14,20	1.013719×10^{3}	-8.412695×10^{2}
46	6.051	3,9,14,20	1.055712×10^{3}	-8.901512×10^{2}
47	6.123	3,9,15,20	1.103198×10^{3}	-9.406120×10^{2}
48	6.166	3,9,15,21	1.146548×10^{3}	-9.926553×10^{2}
49	6.208	3,9,15,22	1.190402×10^{3}	-1.046250×10^{3}
50	6.255	4,10,15,21	1.235897×10^{3}	-1.101458×10^{3}

TABLE IV. Melting temperatures and potential barriers (image potentials being taken into account).

	T_c	Λ	$U_{1,2}$
$N=11$. Orientational melting of the external shell relative to the internal one.	2.5×10^{-7}	40×10^{5}	1.9×10^{-6}
$N=11$. Total melting.	4.0×10^{-3}	250	4.1×10^{-2}
$N=37$. Orientational melting of the external shell relative to the middle one.	8.0×10^{-4}	1250	1.68×10^{-3}
$N=37$. Orientational melting of the middle shell relative to the internal one.	2.6×10^{-3}	385	1.54×10^{-2}
$N=37$. Total melting.	7.5×10^{-3}	133	6.56×10^{-2}

$$U_{\text{ext}}=\gamma\sum_i x_i^2+(2-\gamma)\sum_i y_i^2, \tag{11}$$

where $0\leqslant\gamma\leqslant2$ ($\gamma=1$ corresponds to the isotropic case).

Below we discuss changes of the equilibrium structure of vortex clusters induced by confinement anisotropy. (In this section we do not consider image potentials.) We calculate equilibrium configurations by the method described above (see Sec. III). Now we use polygons inscribed into ellipses (not in circles) as initial configurations.

We have studied configurations in local and global minima of the potential energy for $N=7,11,37$ vortices with a different anisotropy parameter γ in Eq. (11) and found the following effects.

(1) The more anisotropy degree, the more *global minima displace into configurations with a smaller number of particles in the internal shells and with a smaller number of shells.* Shells become ''flat'' and close to polygons, inscribed into ellipses. We must change the definition of the shell given above. Now the largest value of $r_i\sqrt{(2-\gamma)\sin^2\phi_i+\gamma\cos^2\phi_i}$ for particles of each shell must be larger than the smallest value of $r_i\sqrt{(2-\gamma)\sin^2\phi_i+\gamma\cos^2\phi_i}$ for particles being external relative to this shell. (Because of confinement anisotropy the maximal value r_i for particles of each shell may be much larger than the minimal value r_i for particles belonging to the external shell.)

(2) At strong confinement anisotropy an internal shell can have two *tails*, directed along the axis y (if $\gamma<1$, i.e., $\gamma<2-\gamma$) or can simply convert into a *straight line* (in these cases the cluster usually consists of one or two shells). The same rearrangement takes place for the cluster consisting of one shell.

(3) *The more confinement anisotropy, the less number of local minima* the cluster with a given N has. At very strong anisotropy a degree cluster has only one minimum—a straight line.

One can follow the effects described above in Table V.

Let us consider changes of the vortex cluster melting with the increase of the confinement anisotropy degree. One can predict that at sufficiently strong anisotropy of confinement the orientational melting must vanish and the melting becomes one-stage. For the confirmation of this hypothesis we study potential barriers of shells rotation U_2 and of jumps of particles U_1 for the example of a cluster with 37 vortices (see Table VI). It is clear from Sec. V that if barriers of relative shells rotation become larger then barriers of jumps of particles, than one-stage melting occurs. One can see from Table VI that for a small anisotropy degree $\gamma=0.89$ the ratio U_2/U_1 decreases, consequently T_{c_2}/T_{c_1} also decreases, which does not agree with the prediction above. This effect can be explained by the displacement of the potential energy for global minimum vs γ from the configuration 1,6,12,18, close to the triangular lattice fragment, to the configuration 6,12,19, which does not look like a fragment of a triangular lattice. However at further increase of the anisotropy degree

TABLE V. Shell structure and potential energy of clusters of vortices with confinement anisotropy being taken into account. Here Lx means line which consists of x vortices; $2*Ty$ means two tails, each of which consists of y vortices.

Number of particles	Anisotropy parameter γ	Shell fillings	Potential energy U_{pot}
7	1.00	1,6	-7.512442×10^{-1}
7	0.89	1,6	-8.891301×10^{-1}
7	0.67	1,6	-2.136851×10^{0}
7	0.50	1,6	-4.172614×10^{0}
7	0.40	1,6	-6.029061×10^{0}
7	0.33	$l7$	-7.802550×10^{0}
7	0.18	$l7$	-1.416698×10^{1}
11	1.00	3,8	-1.709333×10^{1}
11	0.89	2,9	-1.251753×10^{1}
11	0.67	2,9	-1.566826×10^{1}
11	0.50	11	-2.082752×10^{1}
11	0.40	11	-2.560793×10^{1}
11	0.33	11	-2.983309×10^{1}
11	0.18	$L11$	-4.548732×10^{1}
37	1.00	1,6,12,18	-5.053534×10^{2}
37	0.89	6,12,19	-5.095770×10^{2}
37	0.67	$L4$,13,20	-5.456363×10^{2}
37	0.50	15,22	-6.037877×10^{2}
37	0.40	$9+2*T2$,24	-6.580007×10^{2}
37	0.33	$L9$,28	-7.064780×10^{2}
37	0.18	37	-8.840317×10^{2}
37	0.10	$31+2*T3$	-1.073160×10^{3}
37	0.06	$17+2*T10$	-1.237329×10^{3}
37	0.03	$L37$	-1.468088×10^{3}

TABLE VI. Potential barriers of vortex cluster with $N=37$ with different confinement anisotropy. γ is anisotropy parameter, U_{2a} is barrier of rotation of the external shell relative to the middle shell, U_{2b} is the barrier of rotation of the middle shell relative to the internal shell, U_1 is barrier of the jump of a particle between shells.

γ	U_{2a}	U_{2b}	U_1
1.00	2.31×10^{-3}	1.60×10^{-2}	6.60×10^{-2}
0.89	1.14×10^{-4}	5.84×10^{-2}	5.01×10^{-2}
0.67	1.17×10^{-2}	6.67×10^{-2}	3.04×10^{-2}
0.50	9.47×10^{-2}	—	4.64×10^{-2}

γ rotation barriers become larger than radial ones, which does agree with the prediction above (see Table VI). So for $\gamma=0.67$ in a cluster with 37 vortices only the orientational melting of the external shell relative to the middle one is possible and the orientational melting of the middle shell relative to the internal one is impossible, and for $\gamma=0.50$ the orientational melting is impossible.

To show that melting of the 2D vortex cluster has only one stage for the cases of strong confinement anisotropy we calculated temperature dependences of radial and relative angular deviations for $\gamma=0.50$ [configuration (15,22) in the global minimum of the potential energy]. We found that the dependences of radial and relative angular intrashell and intershell deviations jump at the same temperature $T_c=4.5\times10^{-3}$. That is why we can say that our predictions were true and the melting of a 2D vortex cluster with high anisotropy $\gamma=0.50$ has one stage.

It should be also noted that for very large anisotropy degree of confinement the melting of a cluster does not occur because the cluster becomes a one-dimensional system. That is why *with the increasing of the confinement anisotropy degree two-stage melting changes to one-stage melting and then melting vanishes.*

VIII. CONCLUSIONS

(1) It is shown that two-dimensional microclusters of particles, which are repelled according to a logarithmic law and confined by a parabolic potential, have the shell structure at low temperatures. The configurations of the system in the local and global minima of the potential energy are found. Physical realizations of the considered model are: vortices in a small island of a superconductor or in a rotating vessel with a superfluid, and also electrons in a semiconductor nanostructure surrounded by an environment with small dielectric constant.

(2) The temperature dependences of the potential energy, the radial, and the relative angular intrashell and intershell deviations from equilibrium positions for logarithmic clusters are investigated in detail. As a result the melting of the system is studied. It is shown that the melting has two stages: at first (at lower temperatures) ordered shells start rotating one relative to another, *the orientational melting* of different pairs of shells having different temperatures. At higher temperatures the shell structure disappears. In this connection it would be very interesting to discover experimentally new orientational melting of microclusters of vortices, for example, by observation of vortices using a layer of magneto-optical material, local magnetization of which is studied with the help of a polarizational microscope (in this case observation of reorientation of shells of vortices is possible in a real time) or by scanning tunneling microscope or with the help of decorating. Results of this study can be also applied to the imperfect two-dimensional vortex crystal. There are effects of pinning of a vortex crystal at the boundaries of grains and at the imperfections in the host material. These imperfections may play the role of centers of confinement potential. Short-range order near the imperfections can have the structure of clusters and can melt orientationally prior to the whole crystal melting. For larger microclusters orientational melting takes place only for external pairs of shells due to the triangular structure of large clusters.

(3) The potential barriers of rotation of shells one relative to another occur to be essentially smaller for small microclusters than the barriers corresponding to jumps of a particle from one shell to another but for larger microclusters they are approximately equal. This fact relates to the two-stage melting of a small microcluster, particularly, to the smallness of the temperature of orientational melting in comparison with the total (''radial'') melting of a small microcluster.

(4) We calculated all configurations corresponding to the local and global minima of the potential energy for $N=1,\ldots,50$. Configurations with more vortices in the internal shells become more stable due to image potentials. We found that almost all configurations in the global minima do not change at fixed N and varying R. We investigated the melting and potential barriers in microclusters by taking into account image potentials and found that the two-stage character of melting does not change, but differences between melting temperatures change. These changes are connected with variations of potential barriers of rotation of shells and that of jumps of particles due to image potentials.

(5) We investigated rearrangements of the cluster structure due to different degrees of confinement anisotropy. For small anisotropy global minima displace into configurations with a smaller number of particles in the internal shells and with a smaller number of shells. At strong confinement anisotropy the internal shell can have two *tails*, directed along the long axis or can even convert itself into a *straight line*. If the cluster consists of one shell, it becomes *one-dimensional* as anisotropy rises. Calculation of the barriers of relative rotation of shells and barriers for jumps of particles between shells show that *at some confinement anisotropy orientational melting vanishes* and melting becomes one stage.

ACKNOWLEDGMENTS

This work was partially supported by grants from the INTAS Russian Foundation of Basic Research and ''Physics of Solid Nanostructures.''

*Electronic address: lozovik@isan.troitsk.ru

[1] A. A. Abrikosov, Zh. Eksp. Teor. Fiz. **32**, 1442 (1957).
[2] G. Blatter, M. V. Feigel'man, V. B. Geshkenbein, A. I. Larkin, V. M. Vinokur, Rev. Mod. Phys. **66**, 1125 (1994).
[3] Yu. E. Lozovik, Usp. Fiz. Nauk **153**, 356 (1987).
[4] J. J. Thomson, Philos. Mag. **7**, 238 (1904).
[5] Yu. E. Lozovik, Proc. RAS (Bull. Russ. Acad. Sci. Phys. Ser.) **60**, 85 (1996); Yu. E. Lozovik, and E. A. Rakoch, Pis'ma Zh. Éksp. Teor. Fiz. **65**, 268 (1997) [JETP Lett. **65**, 282 (1997)]; Phys. Lett. A **235**, 55 (1997).
[6] Yu. E. Lozovik, and V. A. Mandelshtam, Phys. Lett. A **145**, 269 (1990); Yu. E. Lozovik, V. A. Mandelshtam, Phys. Lett. A **165**, 469 (1992); Yu. E. Lozovik (unpublished).
[7] F. M. Peeters, V. A. Schweigert, V. M. Bedanov, Physica B **212**, 237 (1995).
[8] Y. Pearl, Appl. Phys. Lett. **5**, 65 (1964).
[9] 3D Coulomb clusters in a confined potential play the role of the physical realization of a 3D Thomson atom (Refs. 3 and 6 see also the 2D case in Refs. 3, and 5–8.
[10] G. B. Hess, Phys. Rev. **161**, 189 (1967).
[11] D. Stauffer, A. L. Fetter, Phys. Rev. **168**, 156 (1968).
[12] L. J. Campbell, R. M. Ziff, Phys. Rev. B **20**, 1886 (1979).
[13] G. E. Volovik, U. Parts, Pis'ma Zh. Eksp. Teor. Fiz. **58**, 826 (1993).
[14] H. Totsuji and J. L. Barrat, Phys. Rev. Lett. **60**, 2484 (1988).
[15] K. Tsuruta, and S. Ichimaru, Phys. Rev. A **48**, 1339 (1993).
[16] Taking into account the ''relaxation'' of positions of particles during the rotation of shells or during the jump of a particle between shells essentially reduces barriers for rotation and for jump. In the opposite case, as calculations show, we have non-realistic, too high values (in the first case this effect is especially too large).